IJCRT.ORG ISSN : 2320-2882

INTERNATIONAL JOURNAL OF CREATIVE RESEARCH THOUGHTS (IJCRT)

An International Open Access, Peer-reviewed, Refereed Journal

Adsorption of CO_2, CH_4, N_2O, and N_2 on MOF-5, MOF-177, and Zeolite 5A

By: Nikita Gupta

Department of Chemistry (Shree Venketeswar University)

Adsorption harmony and energy of CO2, CH4, N2O, and N2 on two newfound adsorbents, metal-natural systems MOF-5 and MOF-177 and one conventional adsorbent, zeolite not entirely set in stone to survey their adequacy for CO2, CH4, and N2O expulsion from air and division of CO2 from CH4 in pressure swing adsorption processes. On all three adsorbents, the volumetric adsorption equilibrium and kinetics data for CO2, CH4, N2O, and N2 were measured at 298K and gas pressures up to 800 Torr. Adsorption balance limits of CO2 and CH4 on each of the three adsorbents were resolved gravimetrically at 298 K and raised pressures (14 bar for CO2 and 100 bar for CH4). The adsorption isotherms were correlated using Henry's law and Langmuir adsorption equilibrium models, and the adsorption kinetic data were analyzed using the traditional micropore diffusion model. The adsorption harmony selectivity was determined from the proportion of Henry's constants, and the adsorbent determination boundary for pressure swing adsorption not entirely set in stone by consolidating the balance selectivity and working limit proportion. Considering the selectivity and adsorbent determination boundary results, zeolite 5A is a superior adsorbent for eliminating CO2 and N2O from air and division of CO2 from CH4, though MOF-177 is the adsorbent of decision for eliminating CH4 from air. Nonetheless, both MOF adsorbents have bigger adsorption capacities with respect to CO2 and CH4 than zeolite 5A at raised pressures, proposing MOF-5 and MOF-177 are better adsorbents for CO2 and CH4 stockpiling. The CH4 adsorption limit of 22 wt.% on MOF-177 at 298K and 100 bar is likely the biggest adsorption take-up of CH4 on any dry adsorbents. The typical diffusivity of CO2, CH4 and N2Oin MOF-5 and MOF-177 is in the request for 10-9 m2/s, when contrasted with 10-11 m2/s for CO2, CH4 and N2O in zeolite 5A. The impacts of gas strain on diffusivity for various adsorabte-adsorbent frameworks were likewise explored.

Introduction

Evacuation of CO2, CH4, and N2O from air and partition of CO2 from CH4 are significant division processes in energy creation and ecological assurance. These divisions can be accomplished in pressure swing adsorption processes assuming reasonable adsorbents with adequately huge selectivity and adsorption limit can be distinguished. Assessment of different adsorbents for their balance and dynamic properties is a powerful method for evaluating reasonable adsorbents for these applications; it additionally adds to better comprehension of essentials of adsorption processes.

With the descant expansion in total populace, headway of industrialization and advances of tech-nologies, utilization of petroleum derivatives has produced expanding measures of ozone depleting substances that have a danger to the climate through an Earth-wide temperature boost impact. Carbon dioxide (CO2) is the principal wellspring of ozone depleting substance that adds to 60% of a dangerous atmospheric deviation impact (1). It was assessed that 82.4% of absolute CO2 was let out of nuclear energy stations (2) and the significant parts of the leftover division was contributed via vehicles. To restrict the CO2 level in the environment, U.S. Branch of Energy

has fostered a guide that requires all petroleum derivative use offices should eliminate the vast majority of CO2 at under 10% expansion in energy administrations by 2012. CO2 discharges to the climate can be diminished in three ways: energy force decrease, carbon power decrease, and carbon catch and sequestration (3). Among these choices, carbon catch and sequestration are presumably the most possible arrangement over the long haul (3, 4). Notwithstanding, the significant expense and low productivity of the partition media (adsorbents, films and so on) are the principal difficulties to carry out this innovation as of now (5). The generally involved strategies for CO2 detachment from vent gases incorporate ammonium ingestion process (6, 7), double soluble base assimilation (8), film division process (9, 10), and adsorption on strong adsorbents (11-20). Adsorption and capacity of CO2 in different nano porous adsorbents have acquired expanding interests as of late and a considerable lot of the few examination papers were distributed to report further developed CO2 adsorption limit. Przepiorski et al. (11) utilized NH3-offered CWZ-35 enacted carbon adsorb CO2 and got a limit of 76 mg/g. Kim et al. (12) showed the CO2 adsorption limit on an amine-treated mesoporous silica to be 1.79 mmol/g at room temperature. Drage et al. (13) announced 3.86 wt.% of CO2 take-up by artificially actuated urea-formaldehyde and melamine-formaldehyde tars. Xu et al. furthermore, Tune et al. (14, 15) impregnated MCM-41 silica adsorbent with Poly ethylamine (PEI) and acquired CO2 limit of 246 mg/g. Fauth et al. (16), Essaki et al. (17) and Kato et al. (18) assessed some lithium-based adsorbents including lithium zirconate and lithium silicate for CO2 partition with a temperature swing approach. Yaghi et al. (19) estimated CO2 adsorption on different Zn-based metal-natural casing works and found that MOF-177 can adsorb 35 mmol/g of CO2 at 45 bar and room temperature.

Regardless of offering less toward a worldwide temperature alteration, methane (CH4) and nitrous oxide (N2O) have more grounded impact as nursery specialists according to unit mass premise (3). Himeno et al. (20) performed CH4 adsorption on different sorts of monetarily accessible initiated carbon and detailed a methane adsorption take-up of 10 mol/kg at 3000 kPa and 273K. Lee et al. (21) tried phenol-based enacted carbons for CH4 adsorption and got an adsorption measure of 8.055 mmol/g at 35.64 bar and 193.15K. Zhou et al. (22) researched the adsorption of CH4 on dry and water-stacked multiwalled carbon nanotube and detailed a CH4 take-up of 8 wt % at 10 MPa and 275 K. A lot higher methane adsorption limit of 30 wt.% on an enacted carbon preloaded with water was likewise gotten by a similar exploration bunch at 10 MPa and 277 K (23). Cavenati et al. (24) announced the adsorption balance limit of CH4 on zeolite 13X of 5.719 mol/kg at 4.725 MPa and 298K. The fundamental uses of eliminating CH4 from air remember air refinement for coal mining and partition of CH4 in biogas produced in garbage removal and biomass maturation locales. Nitrous oxide is accounted for to be a 150-times more grounded ozone harming substance than CO2 (25, 26), it is likewise considered as ozone draining substance. The fundamental wellsprings of N2O delivery to the environment are from nitric corrosive and adiptic corrosive creation offices (27). The critical method for N2O decrease from the tail gases is to deteriorate or lessen it by appropriate impetuses that incorporate zirconia (28), platinum (29, 30), R-manganese sesquioxide (31), and Fe-ZSM-5 zeolite (32-38). As of late, it was shown that bimetallic FER impetuses containing iron and ruthenium increment the synergist movement (39). Synergist disintegration of N2O normally happens at high temperatures and can't recuperate N2O as an important moderate for the development of other fine synthetic substances (40, 41). N2O adsorption on silicalite-1 was performed by Groen et al. who revealed a N2O take-up of 2.5 mol/kg at 273 K (42). Adsorption of N2O was additionally estimated in specific sort of pseudomorphs by Sheep and West (43).

As of late fostered various sorts of zinc-based metal-natural systems (MOF) are viewed as ideal adsorbents inferable from their extremely high unambiguous surface region, tunable pore size and enormous available pore volume (44-48). We have concentrated on hydrogen adsorption harmony and energy on MOF-5 and MOF-177 at different circumstances, assessed their underlying strength, and showed these two MOF adsorbents to be promising adsorbents for hydrogen capacity (49-51), and might want to investigate the practicality of eliminating the ozone depleting substances CO2, CH4 and N2O from different gas streams by adsorption on these two new adsorbents. The target of this work is to decide the adsorption harmony and energy of CO2, CH4, N2O, and N2 on MOF-5, MOF-177, and zeolite 5A; break down the adsorption information with fitting adsorption balance and energy models; and look at the adequacy of eliminating CO2, CH4, and N2O from air, and detachment of CO2 from CH4 by adsorption on MOF-5, MOF-177 and zeolite 5A. This data will be significant for choosing fitting adsorbents for gas partition and purging in a tension swing adsorption process.

Materials and Methods:

The zeolite 5A example assessed in this work was mercifully given by Mr. Li Shenan of Nanjing Treatment facility, SINOPEC, China. It was initially produced for isolating n-paraffin (C10-C13) from lamp oil in a reenacted moving bed, and later improved for oxygen detachment/focus from air in pressure swing adsorption processes.

Synthesis of MOF-5 and MOF-177:

The MOF-5 and MOF-177 examples were blended in our research center following the amalgamation strategies revealed in our past bar libations (49-52). A concise portrayal of the blend methodology is given beneath. For MOF-5 blend, every one of the synthetic compounds were bought from Fisher Logical, and they are of the greatest accessible business immaculateness (99+%, with the exception of zinc nitrate hexahydrate of 98% virtue). 0.832 g of zinc nitrate hexahydrate and 0.176 g of benzene dicarboxylic corrosive were broken up in 20 mL of N,N-dimethylformamide (DEF) under consistent fomentation at surrounding conditions. The subsequent combination was first degassed threefold utilizing the freeze-siphon defrost strategy, and afterward 20 mL response vials were filled for crystallization. The covered vials were quickly placed in a stove (at 85-90°C) for crystallization for around 24 h. Toward the finish of the crystallization step, clear brilliant gems of MOF-5 arose out of the wall and base of the vials. The MOF-5 precious stones were isolated from the response arrangement, washed with DEF to eliminate the unreacted zinc nitrate, and followed by filtration in chloroform. The chloroform cleaning was performed by adding chloroform into 20 mL vials containing the crude MOF-5 precious stones. The vials were covered firmly and returned to the broiler at 70°C for an additional 3 days. Dissolvable in the vials was renewed with new chloroform consistently. After the chloroform treatment, the MOF-5 precious stones transformed from a brilliant variety to straightforward. Since MOF-5 gems are entirely helpless to dampness and air, they must be put away in chloroform or under a vacuum in a Schlenk flagon.

The blend of MOF-177 can be partitioned into two stages: amalgamation of the benzene Tri benzoate (BTB) ligand and development of MOF-177 precious stones. The BTB ligand was orchestrated in our research facility following the systems detailed by Furukawa et al. (48). To create MOF-177, 0.32 g of zinc nitrate hexahydrate and 0.07 g of BTB ligand were disintegrated in 20 mL of dimethyl formamide. The blend was degassed multiple times utilizing the freeze-siphon defrost technique and afterward put away in a 20 mL response vial that was completely loaded up with the combination and covered firmly. The vial was then placed in a broiler at 67°C for 7 days. Toward the finish of this step, clear and straightforward MOF-177 framed and became apparent in the wall as well as on the foundation of the vial. The vial was then taken out from the broiler, tapped, and washed with dimethyl formamide to eliminate the unreacted zinc nitrate. The crude MOF-177 precious stones were then refined by the chloroform treatment process utilized for MOF-5 gem sanitization and put away in chloroform or in a Schlenk jar under vacuum in light of the fact that MOF 177 is vulnerable to sticky air.

Material Characterization:

MOF-5, MOF-177, and zeolite 5A examples were inspected for their stage structure by powder X-beam diffraction (XRD) utilizing a Rigaku Mini flex-II X-beam diffractometer with CuKR emanation, 30 kV/15 Mama current and k§-channel. To inspect the precious stone construction and size of the absorbents, each of the three adsorbent examples were examined with a table-top checking electron magnifying instrument (Hitachi TM-1000). The adsorbents tests were likewise portrayed for their pore textural properties with a Micromeritics pronto 2020 adsorption contraption at 77K. The XRD designs and SEM pictures of MOF-5, MOF-177 and zeolite 5A can be tracked down in Supporting Data (SI) Figures S1 and S2.

Adsorption Measurements.

Adsorption balance and energy of CO2, CH4, N2O, and N2 on the adsorbent examples were estimated volumetrically in a Micromeritics as quickly as possible 2020 adsorption contraption at 298 K and gas pressures up to 800 mmHg. The adsorbate gas was brought into the adsorption framework at a given strain, and the progressions of gas tension with time were recorded and changed over into the transient adsorption sum as an element of time. The transient adsorption takes-up produced the adsorption energy, and the last adsorption sum at the terminal tension decided the adsorption balance sum at a given strain.

Adsorption of CO2 and CH4 at raised pressures was performed gravimetrically in a Robotham attractive sus-benefits balance at 298 K and tensions up 14 bar for CO2 and 100 bar for CH4. The high strain was accomplished by utilizing a blower that is equipped for compacting the adsorbate gas from the chamber strain to a raised tension level. Like any remaining gravimetric gadgets, this equilibrium was additionally pre-analyzed with the clear run of void equilibrium and volume run of test stacked balance to gauge the weight and volume of void example holder and test itself prior to presenting the specific gas of interest. The point by point activity methods for the Rubotherm attractive suspension balance were depicted in our past distributions (50, 51, 53).

Adsorption Theories:

To evaluate the adsorption balance selectivity and anticipate promotion sorption of gas blend from unadulterated part isotherms, the Henry's regulation direct isotherm condition and the Langmuir model were utilized to relate the N2 adsorption on MOF-5 and MOF-177. The Henry's isotherm condition is

$$Q = KP \quad \text{.....(1)}$$

To assess the adsorption harmony selectivity and anticipate promotion sorption of gas combination from unadulterated part isotherms, the Henry's regulation direct isotherm condition and the Langmuir model were utilized to associate the N2 adsorption on MOF-5 and MOF-177. The Henry's isotherm condition is where q is the adsorbed sum per unit weight of adsorbent (wt.%), P is the adsorbate gas tension at harmony (torr), and K is the Henry's regulation consistent (wt.%/torr).

The Langmuir isotherm is figured out as

$$Q = \frac{am+bp}{1+bp} \quad \text{.....(2)}$$

where am (wt.%) and b (torr-1) are the Langmuir isotherm equation parameters. They can be determined from the slope and intercept of a linear Langmuir plot of (1/q) versus (1/P).

Adsorption Equilibrium Selectivity.

To assess the adequacy of an adsorbent for gas partition and filtration like evacuation/detachment of CO2, CH4, N2O from air by adsorption, it is important to realize the adsorbent properties including adsorption limit and selectivity. The adsorption harmony selectivity R12 between parts 1 and 2 is characterized as

$$\alpha = \frac{X1}{X2} * \frac{Y2}{Y1} \approx \frac{K1}{K2} \approx \frac{am1b1}{am2b2} \quad \text{.....(3)}$$

where part 1 is the more grounded adsorbate and 2 is the more vulnerable adsorabte. X1 and X2 are the molar parts of parts 1 and 2 on the adsorbent surface (or in the adsorbed stage), Y1 and Y2 are the molar parts of parts 1 and 2 in the gas stage. am1 and am2 and b1 and b2 are the Langmuir condition constants for parts 1 furthermore, 2. K1 and K2 are the Henry's constants for parts 1 and 2. The harmony selectivity characterized in the abovementioned condition is fundamentally the proportion of the Henry's constants of the two parts, which is the natural selectivity that is as it were legitimate at extremely low gas tension and low adsorption stacking on the adsorbent.

For pressure swing adsorption process, the adsorbent determination boundary S characterized in the accompanying condition is more valuable in adsorbent assessment and choice because it incorporates the proportion of adsorption limit distinction of parts 1 and 2 (54):

$$S = \frac{\Delta q1}{\Delta q2}\alpha 12 \quad \text{.....(4)}$$

where Δq1 and Δq2 are the working capacity that is calculated as the adsorption equilibrium capacity difference at adsorption pressure and desorption pressure for components 1 and 2, respectively.

Adsorption Kinetics:

A traditional micropore dissemination model was applied to extricate the intracrystalline diffusivity for the three gases inside these adsorbents. The partial adsorption take-up (mt/m∞) can be related with the dissemination time consistent (Dc/rc2) by the accompanying condition if the fragmentary adsorption take-up exists in 70-close to 100% (55).

$$1 - \frac{m_t}{m_\infty} \approx \frac{6}{\pi^2} \exp\left(\frac{-\pi^2 D_c t}{r_c^2}\right) \quad \text{.....(5)}$$

The dispersion time constants (Dc/rc 2, s-1) were determined from the incline of a direct plot of ln(1 - (mt/m∞)) versus t (time) at a given strain. Just data of interest with (mt/m∞) more noteworthy than 70% and under close to 100% were utilized for assessing the dispersion time constants. The intracrystalline diffusivity (Dc) of CO2, CH4, and N2O was determined by increasing the dissemination time steady with rc 2 qualities.

Results and Discussion:

Adsorption Isotherms at Pressure up to 800 Torr. Adsorption and desorption balance isotherms of CO2, CH4, also, N2O, and adsorption isotherms of N2 on each of the three adsorbents at 298 K are plotted in Figure 1(a-d), separately. The adsorption and desorption isotherms displayed in these plots essentially follow a similar way, recommending that the adsorption cycle is reversible and the adsorbed atoms can be recuperated during desorption process, if important. It very well may be seen from the isotherm plots that zeolite 5A has the most grounded liking to all gases examined. CO2 take-up on zeolite 5A at 298 K and 800 Torr is about 20.8 wt.%, which is fundamentally higher than the adsorption limit of a few amine-treated adsorbents (11-13). As it were the polyethylamine (PEI) treated MCM-41 adsorbent was answered to have a higher CO2 adsorption limit, yet at the same the reversibility of the desorption was not explored (14, 15). Like CO2 adsorption, adsorption limit of N2O on zeolite 5A is 17.8 wt.% at 298 K and 800 Torr. This adsorption take-up is two times the sum announced in past deals with adsorptive evacuation of nitrous oxide (42, 43). In contrast to CO2 furthermore, N2O adsorption, adsorption of CH4 and N2 on zeolite 5A is on the lower side, 1.35 wt.% of CH4 and 1.58 wt.% of N2 at 298 K and 800 Torr in spite of the fact that zeolite 5A has the most elevated CH4 or N2 adsorption limit among the three adsorbents assessed in this work. Hence, it tends to be presumed that zeolite 5A can specially adsorb CO2 or N2O over CH4 and N2. Between the two MOF adsorbents, MOF-177 displays higher adsorption limits than MOF-5 for CO2 and CH4 adsorption, yet MOF-5 adsorbs more N2O than MOF-177 at comparable circumstances. N2 adsorption isotherms on each of the three adsorbents were likewise estimated to help us to assess the adsorption selectivity and adsorbent choice. This data will permit us to analyze adsorbent adequacy for eliminating CO2, CH4, N2O from air and isolating CO2 from CH4 and other applications. Henry's regulation was utilized to relate the N2 isotherms on MOF-5 and MOF-177 in light of the fact that these two isotherms are fundamentally straight, and Langmuir condition was utilized to fit all isotherms with the exception of the two direct isotherms of N2 on MOF-5 what's more, MOF-177. The Henry's constants and Langmuir condition boundaries were summed up in Table 1.

Adsorption Equilibrium Selectivity and Adsorbent Selection Parameter.

Table 1 sums up the Henry's constants or the result of the Langmuir condition constants (am × b) that is the comparable to the Henry's consistent, the harmony selectivity and the adsorbent choice boundary for various gases on each of the three adsorbents. The adsorbent choice boundaries were determined at adsorption tension of 1 bar and desorption strain of 0.1 bar in this work, which addresses run of the mill vacuum swing adsorption process conditions for gas division what's more, purging. As displayed in Table 1, for eliminating/isolating CO2 from N2 (air), zeolite 5A is the most appropriate adsorbent among the three adsorbents assessed in this work on the grounds that the balance selectivity and adsorbent choice boundary of CO2 over N2 are the most noteworthy for zeolite 5A. Notwithstanding, for CH4 expulsion from air, MOF-177 is better compared to both MOF-5 and zeolite 5A. By and by, zeolite 5A is a preferred adsorbent over both MOF-5 and MOF-177 for eliminating N2O from air and isolating CO2 from CH4 in a strain swing adsorption process.

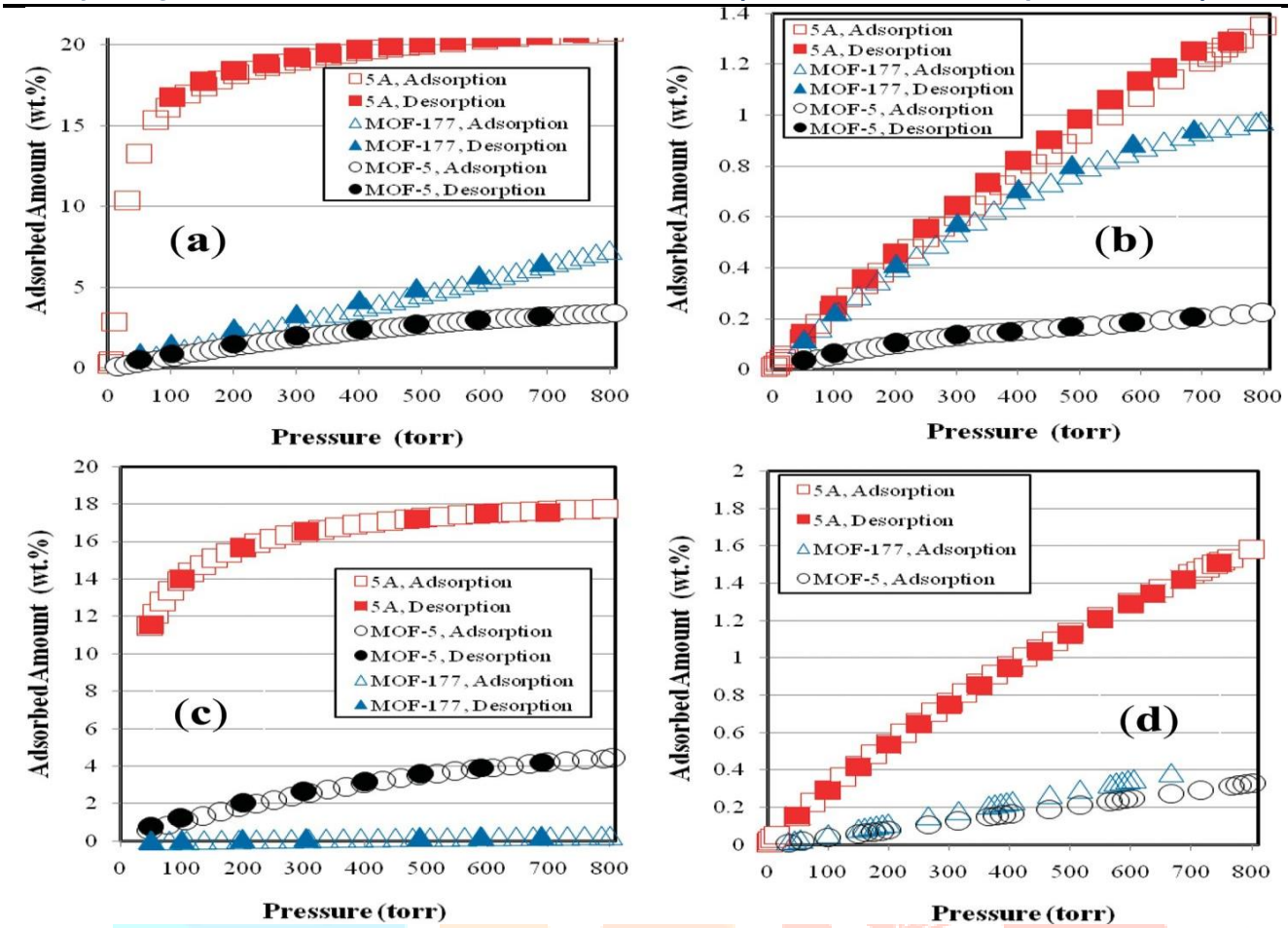

FIGURE 1. Adsorption isotherms of CO_2 (a), CH_4 (b), N_2O (c), and N_2 (d) on MOF-5, MOF-177, and zeolite 5A at 298 K and pressures up to 800 Torr.

Summary of Henry's Constants, Langmuir Equation Parameters, Equilibrium Selectivity and Adsorbent Selection Parameter Calculated from the Pure Component Adsorption Isotherms

Henry's Constants K or $a_m \times b$ (wt.% × torr-1)

	MOF-5	MOF-177	Zerolite-5A
CO_2	13.98 × 0.0005	26.59 × 0.0004	21.14 × 0.033
CH_4	0.45 × 0.001	2.4 × 0.001	2.72 × 0.001
N_2O	8.17 × 0.001	0.67 × 0.001	18.21 × 0.03
N_2	0.0004	0.0006	2.90 × 0.001
Selectivityα_{12}			
CO2/N2	17.48	17.73	240.56
CH4/N2	1.13	4.00	0.94
CH4/N2	20.43	1.12	188.38
CO2/CH	15.53	4.43	256.47
Adsorbent Selection Parameter S (P_{ads} =1 bar, P_{des} =0.1 bar)			
CO2/N2	213.19	233.87	992.77
CH4/N2	0.67	8.45	0.81
N2O/N2	220.29	0.66	708.82
CO2/CH4	318.99	27.68	1232.66

Adsorption Equilibrium at Elevated Pressures:

Table 2shows the adsorption harmony limits of CO2 and CH4 on each of the three adsorbents at 298 K and raised pressures (14 bar for CO2 and 100 bar for CH4). It is seen that the two MOF adsorbents show higher adsorption take-up than zeolite 5A at a raised tension. The Carbon dioxide caught by MOF-5 and MOF-177 at 298 K and 14 bar are 47.97 and 39.69 wt.%, individually, when contrasted with 22 wt.% by zeolite 5A, which is reliable with the CO2 adsorption results acquired on MOF-5 and MOF-177 by Millward and Yaghi (19). CH4 adsorption takes-up by MOF-5 and MOF177 at 298 K and 100 bar are likewise higher than zeolite 5A. Supposedly, the methane adsorption sum (22 wt.%) on MOF-177 at 298K and 100 bar is most likely the most noteworthy methane adsorption limit at any point provided details regarding a dry adsorbent by actual adsorption. The adsorption limits displayed in Table 2 recommend that both MOF-5 and MOF-177 are preferred adsorbents over zeolite 5A for CO2 or CH4 stockpiling at raised pressures albeit the MOFs are not quite as great as zeolite 5A for CO2, CH4 and N2O adsorption at encompassing tensions.

TABLE 2. Summary of Adsorption Equilibrium Capacity of CO2 and CH4 on MOF-5, MOF-177 and Zeolite 5A at 298K and Elevated Pressures

	CO2, 298 K	CH4, 298 K,
adsorbents	14 bar	100 bar
MOF-5	47.98 wt.%	17.15 wt.%
M0F-177	39.27 wt.%	22.03 wt.%
Zeolite 5A	22.27 wt.%	14.31 wt.%

Adsorption Kinetics.

Adsorption energy information of CO2, CH4 and N2O on each of the three adsorbents were gathered at the

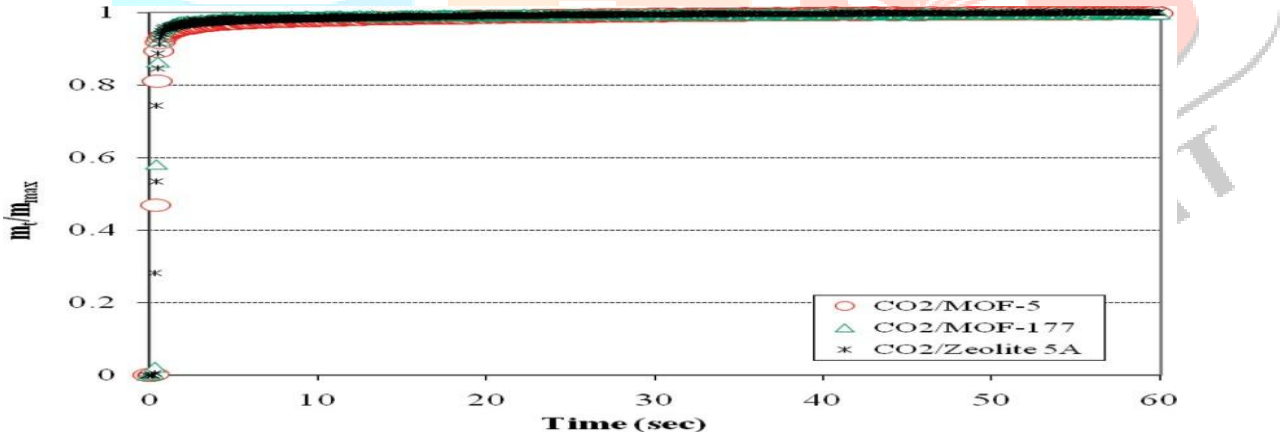

Fig2. Adsorption kinetics of CO_2 on MOF-5,MOF-177, and zeolite 5A at 298 K and pressures up to 800 Torr.

the Micromeritics quickly 2020 adsorption unit. Common dynamic take-up bends of CO2 on all you adsorbents are displayed in Figure 2. Just the partial take-up of CO2 at 800 Torr is plotted, any remaining energy plots are of comparable shape. It is seen from these plots that MOF-5 and MOF-177 arrived at the adsorption immersion level in a more limited stretch of time (inside 5-10 s) as contrasted and zeolite 5A (inside 30-60 s). The sweep rc of 0.5 × 10-6 m for zeolite 5A crystallite, 9.31 × 10-5 m for MOF-5 and 1.2 × roger that m MOF-177 were assessed from their SEM pictures shown in SI Figure S2. The typical diffusivities of these gases on to MOF-5, MOF-177, and zeolite 5A were recorded. The diffusivity of these gases on to both MOFs is in the request of 10-9 m2/s, and for zeolite 5A is in the request for 10-11 m2 /s. The lower size of diffusivity on to zeolite 5A could be added to the lower pore opening of zeolite contrasted with the MOFs. The size of diffusivity in zeolite 5A is reliable with the announced upsides of diffusivities for little gas particles in zeolite 5A (56). The variety of diffusivity with the adjustment of tension is displayed in Figure 3(a-c) for CO2, CH4, and N2O on MOF5, MOF-177 and zeolite 5A, separately. From the plots, clearly the extent of diffusivity affirms a diminishing pattern with the expansion in pressure; aside from

CO2 adsorption on to zeolite 5A, it portrays a converse pattern. The diminishing idea of diffusivity can be credited to the way that the adsorbent pores were to some extent soaked also, hindered at higher adsorption stacking in the higher pressure range leading to languid energy. For the situation of CO2 adsorption on to zeolite 5A, the extremely

high adsorption stacking (up to 18 wt.%) of the adsorbed species on the adsorbent causes a more prominent surface focus coming about in slippage of atoms on to the surfaces. This slippage makes the surface dispersion set in at the higher adsorption stacking at the higher tension and this surface dispersion upgrades the generally speaking intracrystalline diffusivity with the expansion in pressure.

References:

(1) Yamsaki, A. An overview of CO_2 mitigation options for global warmingsEmphasizing CO_2 sequestration options. *J. Chem. Eng. Jpn.* **2003**, *36*, 361–375.
(2) Gray, M. L.; Champagne, K. J.; Fauth, D.; Baltrus, J. P.; Pennline,
H. Performance of immobilized tertiary amine solid sorbents for the capture of carbon dioxide. *Int. J. Greenhouse Gas Control.* **2008**, *2*, 3–8.
(3) Yang, H.; Xu, Z.; Fan, M.; Gupta, R.; Slimane, B.; Bland, A. E.; Wright, I. Progress in carbon dioxide separation and capture: A review. *J. Environ. Sci.* **2008**, *20*, 14–27.
(4) Riahi, K.; Rubin, E. S.; Schrattenholzer, L. Prospects for carbon capture and sequestration technologies assuming their tech- nological learning. *Energy.* **2004**, *29*, 1309–1318.
(5) Halick, P. J. E.; Sayari, A. Applications of pore-expanded mesoporous silica. 5. triamine grafted material with exceptional CO_2 dynamic and equilibrium adsorption performance. *Ind. Eng. Chem. Res.* **2007**, *46*, 446–458.
(6) Resnik, K. P.; Yeh, J. T.; Pennline, H. W. Aqua ammonia process for simultaneous removal of CO_2, SO_2 and NO*x*. *Int. J. Environ. Technol. Manage.* **2004**, *4*, 89–104.
(7) Yeh, J. T.; Resnik, K. P.; Rygle, K.; Pennline, H. W. Semibatch absorption and regeneration studies for CO_2 capture by aqueous ammonia. *Fuel Process. Technol.* **2005**, *86*, 1533–1546.
(8) Huang, H, P.; Shi, Y.; Li, W.; Chang, S. G. Dual alkali approaches for the capture and separation of CO_2. *Energy Fuels.* **2001**, *15*, 263–268.
(9) Damle, A. S.; Dorchak, T. P. Recovery of carbon dioxide in advanced fossil energy conversion processes using a membrane reactor. *J. Energy Environ. Res.* **2001**, *1*, 77–89.
(10) Shekhawat, D.; Luebke, D. R.; Pennline, H. W. A review of carbon dioxide selective membranessA topical report. *National Energy Technology Laboratory*, United States Department of Energy. 2003.
(11) Przepio'rski, J.; Skrodzewicz, M.; Morawski, A. W. High tem- perature ammonia treatment of activated carbon for enhance- ment of CO_2 adsorption. *Appl. Sur. Sci.* **2004**, *225*, 235–242.
(12) Kim, S. N.; Son, W. J.; Choi, J. S.; Ahn, W. S. CO_2 adsorption using amine-functionalized mesoporous silica prepared via anionic surfactant-mediated synthesis. *Microporous Mesoporous Mater.* **2008**, *115*, 497–503.
(13) Drage, T. C.; Arenillas, A.; Smith, K. M.; Pevida, C.; Piippo, S.; Snape, C. E. Preparation of carbon dioxide adsorbents from the chemical activation of urea-formaldehyde and melamine- formaldehyde resins. *Fuel.* **2006**, *86*, 22–31.
(14) Xu, X.; Song, C. S.; Andresen, J. M.; Miller, B. G.; Scaroni, A. W. Novel polyethyleneimine-modified mesoporous molecular sieve Of MCM-41 type as adsorbent for CO_2 capture. *Energy Fuels.* **2002**, *16*, 1463–1469.
(15) Xu, X.; Song, C.; Miller, B. G.; Scaroni, A. W. Adsorption separation of carbon dioxide from flue gas of natural gasfired boiler by a novel nanoporous "molecular basket" adsorbent. *Fuel Process. Technol.* **2005**, *86*, 1457–1472.
(16) Fauth, D. J.; Frommell, E. A.; Hoffman, J. S.; Reasbeck, R. P.; Pennline, H. W. Eutectic salt promoted lithium zirconate: Novel high temperature sorbent for CO_2 capture. *Fuel Process. Technol.* **2005**, *86*, 1503–1521.
(17) Essaki, K.; Nakagawa, K.; Kato, M.; Uemoto, H. CO_2 absorption by lithium silicate at room temperature. *J. Chem. Eng. Jpn.* **2004**, *37*, 772–777.
(18) Kato, M.; Nakagawa, K.; Essaki, K.; Maezawa, Y.; Takeda, S.; Kogo, R.; Hagiwara, Y. Novel CO_2 absorbents using lithium containing oxide. *Intl. J. Appl. Ceramic Technol.* **2005**, *2*, 467– 475.
(19) Millward, A. R.; Yaghi, O. M. Metal-organic frameworks with exceptionally high capacity for storage of carbon dioxide at room temperature. *J. Am. Chem. Soc.* **2005**, *127*, 17998–17999.
(20) Himeno, S.; Komatsu, T.; Fujita, S. High-pressure adsorption equilibria of methane and carbon dioxide on several activated carbons. *J. Chem. Eng. Data* **2005**, *50*, 369–376.
(21) Lee, J. W.; Balathanigaimani, M. S.; Kang, H. C.; Shim, W. G.; Kim, C.; Moon, H. Methane storage on phenol-based activated carbons at (293.15, 303.15, and 313.15) K. *J. Chem. Eng. Data* **2007**, *52*, 66–70.
(22) Zhou, L.; Sun, Y.; Yang, Z.; Zhou, Y. Hydrogen and methane sorption in dry and water-loaded multiwall

carbon nanotubes.
J. Colloid Interface Sci. **2005**, *289*, 347–351.
(23) Zhou, L.; Sun, Y.; Zhou, Y. Enhancement of methane storage on activated carbon by preadsorbed water. *AIChE J.* **2002**, *48*, 2412– 2416.
(24) Cavenati, S.; Grande, C. A.; Rodrigues, A. E. Adsorption equilibrium of methane, carbon dioxide, and nitrogen on zeolite 13X at high pressures. *J. Chem. Eng. Data* **2004**, *49*, 1095–1101.
(25) Rodhe, H. A. comparison of the contribution of various gases to the greenhouse effect. *Science.* **1990**, *248*, 1217–1219.
(26) Centi, G.; Perathoner, S.; Vanazza, F. Catalytic control of non- CO_2 greenhouse gases. *Chemtech* **1999**, *12*, 48–55.
(27) Groen, J. C.; Ramı´rez, J. P.; Zhu, W. Adsorption of nitrous oxide on silicalite-1. *J. Chem. Eng. Data* **2002**, *47*, 587–589.
(28) Miller, T. M.; Grassian, V. H. Environmental catalysis: adsorption and decomposition of nitrous oxide on zirconia. *J. Am. Chem. Soc.* **1995**, *117*, 10969–10975.
(29) Redmoxd, J. P. Kinetics of the low pressure nitrous oxide decomposition on a platinum filament. *J. Phys. Chem.* **1963**, *67*, 788–793.
(30) Watanabe, K.; Kokalj, A.; Inokuchi, Y.; Rzeznicka, I.; Ohshimo, K.; Nobuyuki, Nishi; Matsushima, T. Orientation of nitrous oxide on palladium(1 1 0) by STM. *Chem. Phys. Lett.* **2005**, *406*, 474– 478.
(31) Rheaume, L.; Parravano, G. Decomposition kinetics of nitrous oxide on R-manganese sesquioxide. *J. Phys. Chem.* **1959**, *63*, 264–268.
(32) Kogel, M.; Abu-Zied, B. M.; Schwefer, M.; Turek, T. The effect of NO_x on the catalytic decomposition of nitrous oxide over Fe-MFI zeolites. *Catal. Commun.* **2001**, *2*, 273–276.
(33) Perez-Ramirez, J.; Kapteijn, F.; Mul, G.; Moulijn, J. A. Superior performance of *ex*-framework FeZSM-5 in direct N_2O decom- position in tail-gases from nitric acid plants. *Chem. Commun.* **2001**, 693–694.
(34) Perez-Ramirez, J.; Kapteijn, F.; Mul, G.; Moulijn, J. A. Highly active SO_2-resistant ex-framework FeMFI catalysts for direct N_2O decomposition. *Appl. Catal., B* **2002**, *35*, 227–232.
(35) Guzman-Vargas, A. G.; Delahay, G.; Coq, B. Catalytic decom- position of N_2O and catalytic reduction of N_2O and N_2O + NO by NH_3 in the presence of O_2 over Fe-zeolite. *Appl. Catal., B* **2003**, *42*, 369–379.
(36) Pieterse, J. A.Z.; Booneveld, S.; van den Brink, R. W. Evaluation of Fe-zeolite catalysts prepared by different methods for the decomposition of N_2O. *Appl. Catal., B* **2004**, *51*, 215–228.
(37) Sobolev, V. I.; Panov, G. I. A. S.; Kharitonov, A. S.; Romannikov,
V. N.; Volodin, A. M.; Ione, K. G. Catalytic properties of ZSM-5 zeolites in N_2O decomposition: The role of iron. *J. Catal.* **1993**, *139*, 435–443.
(38) Panov, G. I.; Uriarte, A. K.; Rodkin, M. A.; Sobolev, V. I. Generation of active oxygen species on solid surfaces. Opportunity for novel oxidation technologies over zeolites. *Catal. Today.* **1998**, *41*, 365–385.
(39) Pieterse, J. A. Z.; Mul, G.; Melian-Cabrera, I.; van den Brink,
R. W. Synergy between metals in bimetallic zeolite supported catalyst for NO-promoted N_2O decomposition. *Catal. Lett.* **2005**, *99*, 41–44.
(40) Hoelderich, W. Environmentally benign manufacturing of fine and intermediate chemicals. *Catal. Today.* **2000**, *62*, 115–130.
(41) Panov, G. I. Advances in oxidation catalysis; oxidation of benzene to phenol by nitrous oxide. *Cattech* **2000**, *4*, 18–31.
(42) Groen, J. C.; Pe´rez-Ramı´rez, J.; Zhu, W. Adsorption of nitrous oxide on silicalite-1. *J. Chem. Eng. Data* **2002**, *47*, 587–589.
(43) Lamb, A. B.; West, C. D. The adsorption of nitrous oxide on certain pseudomorphs. *J. Am. Chem. Soc.* **1940**, *62*, 3176–3180.
(44) Wong-Foy, A. G.; Matzger, A. J.; Yaghi, O. M. Exceptional H_2 saturation in microporous metal-organic frameworks. *J. Am. Chem. Soc.* **2006**, *128*, 3494–3495.
(45) Rowsell, J. L. C.; Yaghi, O. M. Strategies for hydrogen storage in metal organic frameworks. *Angew. Chem., Int. Ed.* **2005**, *44*, 4670–4679.
(46) Furukawa, H.; Miller, M. A.; Yaghi, O. M. Independent verification of the saturation hydrogen uptake in MOF-177 and establish- ment of a benchmark for hydrogen adsorption in metal-organic frameworks. *J. Mater. Chem.* **2007**, *17*, 3197–3204.
(47) Li, Y.; Yang, R. T. Gas adsorption and storage in metal-organic framework MOF-177. *Langmuir.* **2007**, *23*,

12937–12944.
(48) Panella, B.; Hirscher, M.; Putter, H.; Muller, U. Hydrogen adsorption in metal-organic frameworks: Cu-MOFs and Zn- MOFs compared. *Adv. Funct. Mater.* **2006**, *16*, 520–524.
(49) Saha, D.; Deng, S.; Yang, Z. Hydrogen adsorption on metal organic framework (MOF-5) synthesized by DMF approach. *J. Porous Mater.* **2009**, *16*, 141–149.
(50) Saha, D.; Wei, Z.; Deng, S. Equilibrium, kinetics and enthalpy of hydrogen adsorption in MOF-177. *Intl. J. Hydrogen Energy.* **2008**, *33*, 7479–7488.
(51) Saha, D.; Wei, Z.; Deng, S. Hydrogen adsorption equilibrium and kinetics in metal-organic framework (MOF-5) synthesized